

## Electronic-structure evolution through the metal-insulator transition in $R\text{NiO}_3$

I. Vobornik, L. Perfetti, M. Zacchigna, M. Grioni, and G. Margaritondo  
*Institut de Physique Appliquée, Ecole Polytechnique Fédérale, CH-1015 Lausanne, Switzerland*

J. Mesot and M. Medarde  
*Materials Science Division, Argonne National Laboratory, Argonne, Illinois 60439-4845*

P. Lacorre  
*Laboratoire des Fluorures, UPRES-A CNRS 6010, Université du Maine, F-72017 Le Mans Cedex 9, France*  
 (Received 19 April 1999; revised manuscript received 22 May 1999)

We performed a photoemission investigation of the electronic structure of  $\text{PrNiO}_3$  and  $\text{NdNiO}_3$  through the first order (paramagnetic) metal to (antiferromagnetic) insulator transition. Surprisingly, the data reveal a temperature-dependent loss of spectral weight near the chemical potential, which extends well below the coincident metal-insulator ( $T_{MI}$ ) and magnetic ( $T_{Néel}$ ) transition temperatures. This is in contrast with the behavior in  $\text{SmNiO}_3$  and  $\text{EuNiO}_3$ , where the two transitions are separate. The spectral properties clearly indicate two distinct regimes for  $R\text{NiO}_3$  with  $T_{MI}=T_{Néel}$  and  $T_{MI}>T_{Néel}$ . [S0163-1829(99)51936-X]

The transition metal oxides exhibit a fascinating variety of physical properties, ranging from magnetism, to high- $T_c$  superconductivity, and to the recently discovered colossal magnetoresistance. One peculiar and still elusive feature of these strongly correlated materials is the occurrence of metal-insulator (MI) transitions, induced for instance by varying the carrier concentration (doping) or by applying external pressure.<sup>1,2</sup> These phenomena are controlled by a complex interplay of various parameters, including the bandwidth ( $W$ ), the charge-transfer energy ( $\Delta$ ) and the Coulomb repulsion energy ( $U$ ). Depending on the relative size of these parameters, the system can be a metal ( $W>U,\Delta$ ), or an insulator. One further distinguishes between charge-transfer ( $U>\Delta$ ) and Mott-Hubbard ( $U<\Delta$ ) insulators, according to the Zaanen-Sawatzky-Allen scheme.<sup>3</sup>

The rare-earth nickelates  $R\text{NiO}_3$  ( $R$ =rare earth different from La) are a rather unique system where the MI transition requires neither electron nor hole doping. They crystallize in an orthorhombically distorted perovskite structure of the  $\text{GdFeO}_3$  type ( $Pbnm$  space group),<sup>4</sup> and the degree of distortion depends on the size of the  $R$  ion placed between eight  $\text{NiO}_6$  octahedra. The consequence of increased distortion is a reduced Ni-O-Ni interaction and therefore a reduced bandwidth, which eventually leads to electron localization at low temperature and the formation of a (charge transfer) band gap.<sup>5</sup> The MI transition is of the first order, and the transition temperature ( $T_{MI}$ ) is a linear function of the cosine of the tilt angle between  $\text{NiO}_6$  octahedra.<sup>6</sup>

In members of the  $R\text{NiO}_3$  series with larger  $R$  ions ( $R$ =Pr, Nd) the MI transition is accompanied by an antiferromagnetic (AF) ordering of the Ni sublattice. For smaller  $R$  ions ( $R$ =Sm, Eu), the MI and magnetic transitions are separate, and the AF ordering temperature ( $T_{Néel}$ ) is lower than  $T_{MI}$ . Neutron diffraction experiments on powder samples indicate a peculiar (antiferro-) magnetic ground state with an alternation of ferromagnetic and antiferromagnetic couplings between nearest neighbor  $\text{Ni}^{3+}$  ions.<sup>7</sup> This magnetic structure may result from an ordering of the Ni  $3d$  orbitals, yield-

ing the observed alternation of positive and negative exchange interactions.<sup>7,8</sup> Recent x-ray and neutron diffraction data have indicated the presence of charge ordering in  $\text{YNiO}_3$ , which is also compatible with the arrangement of Ni spins.<sup>9</sup> This complex magnetic structure has initially been interpreted in terms of a commensurate [ $\mathbf{k}=(1/2,0,1/2)$ ] spin-density wave and, quite naturally, the MI transition has been associated with a magnetic instability.<sup>7</sup> More recently, however, the observation of a giant  $^{16}\text{O}$ - $^{18}\text{O}$  isotope effect at the transition in  $R\text{NiO}_3$ ,  $R$ =Pr, Nd, Sm, Eu,<sup>6</sup> and of charge ordering in  $\text{YNiO}_3$ ,<sup>9</sup> established the importance of the electron-lattice interactions both in compounds with  $T_{Néel}=T_{MI}$  and  $T_{Néel}\neq T_{MI}$ .

While changes in the structural and magnetic properties upon the transition were extensively studied, not much is known about the corresponding changes in the electronic structure. A better knowledge of the electronic structure evolution at a metal-insulator transition in correlated systems is one of the outstanding goals of solid state spectroscopy. It is also a prerequisite for understanding even subtler phenomena, such as the superconductivity in the cuprates. This goal motivated our investigation of selected  $R\text{NiO}_3$  compounds. We report here a high-resolution photoemission (PES) investigation of  $\text{PrNiO}_3$ ,  $\text{NdNiO}_3$ , electron and hole doped  $\text{NdNiO}_3$ ,  $\text{SmNiO}_3$ , and  $\text{EuNiO}_3$ . We find that when  $T_{MI}=T_{Néel}$  (Pr and Nd compounds) the spectral weight within 0.3 eV of the Fermi energy ( $E_F$ ) continuously decreases below  $T_{MI}$  down to the lowest temperatures probed ( $T/T_{MI}\approx 0.5$ ). This trend is doping independent. We observe a different behavior in  $\text{SmNiO}_3$  and  $\text{EuNiO}_3$ , where  $T_{MI}>T_{Néel}$ . Our results reflect the existence of two distinct regimes in the  $R\text{NiO}_3$  family, determined by the relation between the two critical temperatures,  $T_{MI}$  and  $T_{Néel}$ .

Polycrystalline  $\text{PrNiO}_3$ ,  $\text{NdNiO}_3$ ,  $\text{SmNiO}_3$ , and  $\text{EuNiO}_3$  samples were prepared and characterized as described in a previous work.<sup>10</sup> The transition temperature is lowered upon hole or electron doping;<sup>11</sup> the sample with 1%  $\text{Ca}^{2+}$  replacing  $\text{Nd}^{3+}$  in  $\text{NdNiO}_3$  has  $T_{MI}$  of 175 K, while the one with

TABLE I. Metal-insulator temperatures, Néel temperatures, and virtual Néel temperatures for the investigated  $R\text{NiO}_3$  systems.

$R\text{NiO}_3$	$T_{MI}$ (K)	$T_{Néel}$ (K)	$T_N^*$ (K)
$\text{PrNiO}_3$	130	130	257
$\text{Nd}_{0.99}\text{Ca}_{0.01}\text{NiO}_3$	175	Not reported	Not reported
$\text{Nd}_{0.98}\text{Ce}_{0.02}\text{NiO}_3$	191	Not reported	Not reported
$\text{NdNiO}_3$	200	200	250
$\text{SmNiO}_3$	400	230	
$\text{EuNiO}_3$	480	220	

2%  $\text{Ce}^{4+}$  has  $T_{MI}$  of 191 K (see Table I). The photoemission measurements were performed using unpolarized photons of 21.2 eV (He I) and 1486.6 eV ( $\text{AlK}_{\alpha}$ ) and a Scienta 300 hemispherical electrostatic energy analyzer. The resolution was 0.3 eV for the  $\text{AlK}_{\alpha}$  data and 20 meV for the data taken with the HeI radiation. Clean sample surfaces were obtained by scraping. The base experimental pressure was  $2 \times 10^{-10}$  torr.

The spectrum of  $\text{PrNiO}_3$  (Fig. 1) displays the main valence band feature of mixed O  $2p$  and Ni  $3d$  character at  $\sim 5$  eV, and Pr  $4f$  states at  $\sim 1$  eV.<sup>12</sup> Here we are mainly concerned with the low energy excitations, which are involved in and directly affected by the MI transition. This is illustrated in the inset to the first panel, where the close-up of the raw valence band data at 210 K (metallic state) and at  $\sim 70$  K (insulating state) is presented. The data clearly indicate a transfer of the spectral weight from lower to higher binding energies within 0.6 eV below  $E_F$ . The remaining panels of Fig. 1 present a summary of the temperature-dependent data near  $E_F$  for the various compounds. The spectra are normalized at 0.3 eV binding energy—the energy where the high- and low-temperature spectra (inset) intersect.<sup>13</sup> In both the Pr and Nd (either pure or doped) compounds, the spectral intensity drops at  $T_{MI}$ , and further decreases down to the lowest temperatures (72–73 K for  $\text{NdNiO}_3$  and 60 K for  $\text{PrNiO}_3$ ). For  $\text{SmNiO}_3$  and  $\text{EuNiO}_3$ , we could not explore the MI transition which occurs outside

the temperature range of our apparatus. Yet, we could probe the electronic properties up to  $T/T_{MI}=0.97$  for  $\text{SmNiO}_3$  and  $T/T_{MI}=0.82$  for  $\text{EuNiO}_3$ . We found no changes in the spectra from the highest temperature down to 72 K.

A detailed analysis of Fig. 1 indicates that, for all samples, the spectra saturate to an identical low-temperature line shape at 60–70 K.<sup>14</sup> Therefore, to quantify the spectral changes we considered difference curves obtained by subtracting the lowest temperature spectrum from the higher temperature spectra. An example of this procedure is shown in Fig. 2(a). The dashed area is directly related to the temperature-driven change in the density of states. As illustrated in Fig. 2(b), this area changes rapidly just below  $T_{MI}$ , but continues to decrease as temperature decreases. Hysteresis effects, observed in transport measurements,<sup>15,16</sup> were negligible, and within the error bars. Plotting these intensities versus the reduced temperature  $T/T_{MI}$  [Fig. 2(c)], reveals a universal temperature dependence. By contrast,  $\text{SmNiO}_3$  and  $\text{EuNiO}_3$  exhibit a completely different temperature evolution. In Fig. 2(d), we compare the results of our analysis for  $\text{NdNiO}_3$  with the estimated number of electrons affected by the transition ( $N_{eff}$ ) derived from optical conductivity.<sup>17</sup> The two data sets show a qualitatively similar evolution with temperature. The analogy of the PES and optical results is important because, unlike photoemission, optics is a bulk sensitive technique, free from possible spurious surface effects. The observed spectral evolution therefore indicates corresponding intrinsic changes in the electronic structure of  $\text{PrNiO}_3$  and  $\text{NdNiO}_3$  at the MI transition.

Resistivity measurements in this family of oxides reveal a low-temperature activation energy  $2\Delta=20\text{--}25$  meV ( $\sim k_B T_{MI}$ ) in the insulating phase.<sup>15,18</sup> In PES, the expected fingerprint of the opening of such a gap is a shift of the spectral leading edge and zero intensity at  $E_F$ . The finite experimental resolution, however, may modify this picture. A finite intensity at  $E_F$  in the lowest temperature spectra of Fig. 1 rules out a gap symmetric about  $E_F$  of size  $2\Delta$ , but is compatible with  $E_F$  being close (1–3 meV) to the top of the valence band. More importantly, the spectra of Fig. 1 indi-

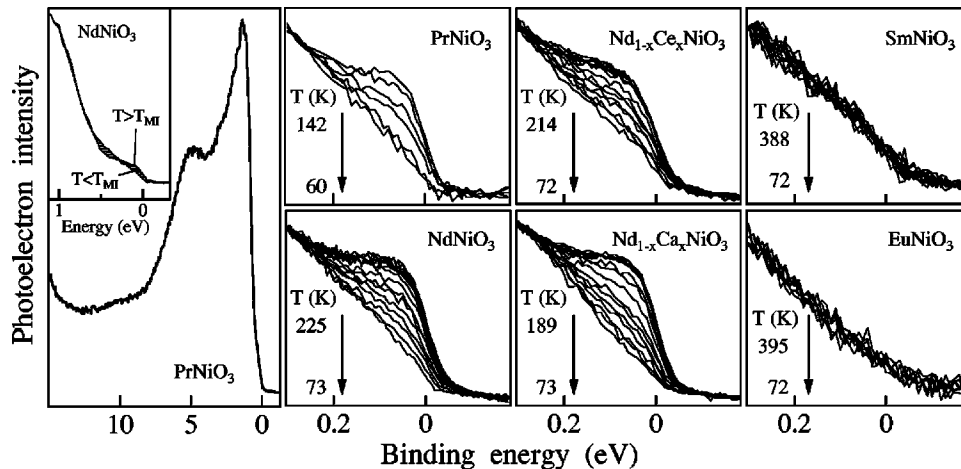


FIG. 1. First panel: Valence band of  $\text{PrNiO}_3$  ( $h\nu=1486.6$  eV); Inset: The zoom-in into the energy interval of  $\sim 1$  eV of  $E_F$  ( $\text{NdNiO}_3$  with  $h\nu=21.2$  eV) showing the spectral weight transfer to higher binding energies below  $T_{MI}$ ; Remaining panels: spectra recorded at different temperatures for  $\text{PrNiO}_3$ ,  $\text{NdNiO}_3$ , electron doped  $\text{Nd}_{0.98}\text{Ce}_{0.02}\text{NiO}_3$ , hole doped  $\text{Nd}_{0.99}\text{Ca}_{0.01}\text{NiO}_3$ ,  $\text{SmNiO}_3$ , and  $\text{EuNiO}_3$  ( $h\nu=21.2$  eV).

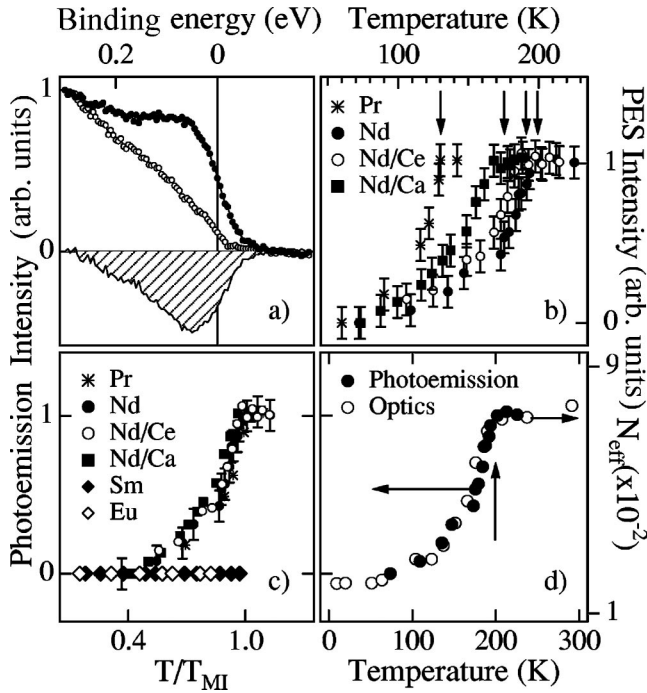


FIG. 2. (a) PES spectra of NdNiO<sub>3</sub> at 200 K (full symbols) and 73 K (open symbols) together with their difference. (b) Temperature dependence of the integrated area of the difference curves for PrNiO<sub>3</sub>, NdNiO<sub>3</sub>, Nd<sub>0.98</sub>Ce<sub>0.02</sub>NiO<sub>3</sub>, Nd<sub>0.99</sub>Ca<sub>0.01</sub>NiO<sub>3</sub>, normalized to the maximum value. (c) The same as (b) versus the reduced temperature ( $T/T_{MI}$ ) and together with the results for SmNiO<sub>3</sub> and EuNiO<sub>3</sub>. (d) The optics result from Katsufuji *et al.* (open symbols; right axis) together with our result from (b) for NdNiO<sub>3</sub> (closed symbols; left axis). The vertical arrows mark the MI transition temperatures.

cate that spectral changes occur over a much larger energy scale of 600 meV ( $\sim 30$  times larger than the gap). This is a strong indication that correlation effects are important in these materials.

In agreement with the above conclusion, a one-electron picture, with corresponding photoemission cross sections taken into account, fails to give an explanation for the observed spectral weight transfer.<sup>19</sup> An alternative approach, which explicitly includes correlation effects, was proposed in Ref. 19, based on an analysis of the core-level spectra in PrNiO<sub>3</sub>.<sup>12</sup> This analysis showed that PrNiO<sub>3</sub> has a mixed  $d^7$ ,  $d^8\bar{L}$  and  $d^9\bar{L}^2$  ground state ( $\bar{L}$  stands for a hole in the O  $2p$  orbitals), while the first ionization state has mainly  $d^7\bar{L}$ ,  $d^8\bar{L}^2$  character. In the insulating state, a reduced covalency suppresses some of these transitions. A reduction of spectral weight at  $T_{MI}$  is then a natural consequence of a reduced covalency. However, it is not clear why the spectral properties should change further with temperature decreasing below  $T_{MI}$ . Alternatively, the spectral weight reduction could be related to changes in the electronic structure induced by the lattice anomaly. Neutron scattering experiments showed that changes in the lattice parameters are limited to 10 K below  $T_{MI}$ .<sup>20</sup> This is in contrast with the PES data, which exhibit a clear temperature dependence to at least  $T \approx 0.5T_{MI}$  [Fig. 2(c)].

Spectral weight transfer over a broad energy region was observed in photoemission studies of manganite systems.<sup>21,22</sup>

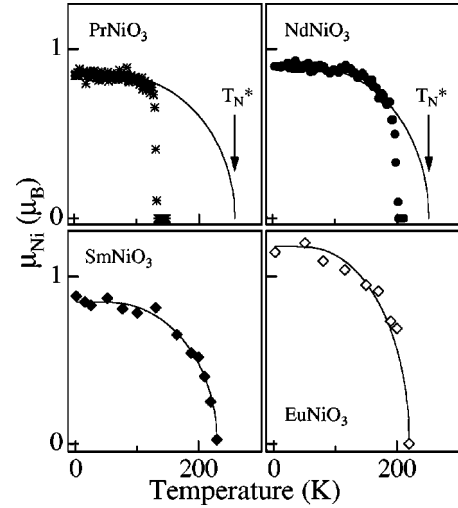


FIG. 3. The evolution of the Ni magnetic moments with temperature for PrNiO<sub>3</sub>, NdNiO<sub>3</sub>, SmNiO<sub>3</sub>, and EuNiO<sub>3</sub>. The lines are an attempt to fit the data with Brillouin function. The arrows mark the virtual Néel temperatures ( $T_N^*$ ) for PrNiO<sub>3</sub> and NdNiO<sub>3</sub>.

In Pr<sub>0.5</sub>Sr<sub>0.5</sub>MnO<sub>3</sub> it is linked with the charge ordering<sup>23,24</sup> that sets in at  $T_{MI}$ .<sup>22</sup> Unlike PrNiO<sub>3</sub> and NdNiO<sub>3</sub>, the spectral weight transfer in Pr<sub>0.5</sub>Sr<sub>0.5</sub>MnO<sub>3</sub> is abrupt and occurs at the charge-ordering temperature  $T_{MI}$ . On the other hand, the temperature-dependent optical conductivity of both NdNiO<sub>3</sub> and of the charge-ordering nickelate La<sub>1.67</sub>Sr<sub>0.33</sub>NiO<sub>4</sub> exhibits a spectral weight transfer and a gap, which follows a BCS-like behavior below  $T_{MI}$ .<sup>17,25</sup> In NdNiO<sub>3</sub>, this was initially taken as an evidence in favor of a magnetic origin of the MI transition, driven by the spin-density-wave instability.<sup>17</sup> The temperature dependence of the gap in La<sub>1.67</sub>Sr<sub>0.33</sub>NiO<sub>4</sub> suggests, however, the formation of a charge-density wave, consistent with charge ordering. The recent observation of charge ordering in YNiO<sub>3</sub>,<sup>9</sup> as well as the giant isotope effect in various members of RNiO<sub>3</sub>,<sup>6</sup> undermines a role of magnetism at the MI transition in this oxide family. The BCS gap evolution in both NdNiO<sub>3</sub> and La<sub>1.67</sub>Sr<sub>0.33</sub>NiO<sub>4</sub> therefore makes it tempting to associate the spectral weight changes with the occurrence of charge ordering. However, this scenario does not clarify why the materials with  $T_{MI} = T_{Néel}$  and  $T_{MI} > T_{Néel}$  exhibit a qualitatively different behavior or what would be the origin of different temperature dependencies of the spectral weight transfer in Pr and Nd nickelates and charge-ordering manganites.

The unexpected temperature dependence in PrNiO<sub>3</sub> and NdNiO<sub>3</sub>, and the distinctly different behavior of SmNiO<sub>3</sub> and EuNiO<sub>3</sub>, suggest a correlation between electronic and magnetic properties. This is supported by the analysis of the temperature-dependent magnetization curves of Fig. 3.<sup>4,8</sup> In SmNiO<sub>3</sub> and EuNiO<sub>3</sub>, where the magnetic and electronic transitions are separated,<sup>5</sup> a Brillouin function gives an excellent fit to the data.<sup>4</sup> On the contrary, the normal Brillouin-type behavior is strongly violated in both PrNiO<sub>3</sub> and NdNiO<sub>3</sub>. The Ni moments saturate to approximately  $1 \mu_B$  immediately below  $T_{Néel}$ , suggesting the existence of a virtual Néel temperature<sup>4</sup>  $T_N^* > T_{Néel} = T_{MI}$  (Table I). In this way, as PES, magnetization also clearly distinguishes two regimes:  $T_{MI} = T_{Néel}$  and  $T_{MI} > T_{Néel}$ . Further evidence for the possible role played by magnetism in the transition is

suggested by recent magnetotransport results.<sup>26</sup> The data show that at low temperatures, the magnetoresistance changes sign in the compounds where  $T_{MI}=T_{Néel}$ , but not in the compounds where the two transitions are separate. All this suggests that the temperature dependence of the gap in members of the  $RNiO_3$  family, where  $T_{MI}=T_{Néel}$ , is strongly correlated with the concomitant formation of the ordered magnetic state. This is a surprising result. The MI transition is not triggered by the magnetic transition, and it would be natural to assume that the temperature dependence of the electronic structure should also be independent of magnetism. Our results alone cannot determine to which extent (if any) magnetism is involved in the transition in  $RNiO_3$  with  $T_{MI}=T_{Néel}$ . However, they experimentally establish a clear distinction between the nickelates with  $T_{MI}=T_{Néel}$  and  $T_{MI}>T_{Néel}$ . This correlation between spectral and magnetic properties calls for further theoretical consideration.

In summary, we investigated the changes induced by the

MI transition in the electronic structure of  $RNiO_3$ . In systems where  $T_{MI}=T_{Néel}$ , we observe a continuous spectral weight transfer away from the chemical potential below  $T_{MI}$  (in the insulating phase). This temperature-driven spectral evolution is in contrast with the first order character of the transition. Although recent results discarded magnetism as the driving force for the transition, our data indicate a possible interplay between electronic and magnetic degrees of freedom when  $T_{MI}=T_{Néel}$ . They also further substantiate the qualitative difference between systems where  $T_{MI}=T_{Néel}$  and  $T_{MI}>T_{Néel}$ . Any future model of the transition in  $RNiO_3$  will have to address these experimental facts.

This work was supported by the Fond National Suisse de la Recherche Scientifique and by the Ecole Polytechnique Fédérale de Lausanne. We gratefully acknowledge fruitful discussions with Dr. Laszlo Forró.

- 
- <sup>1</sup>M. Imada, A. Fujimori, and Y. Tokura, *Rev. Mod. Phys.* **70**, 1039 (1998).
- <sup>2</sup>F. Gebhard, *The Mott Metal-Insulator Transitions* (Springer, Berlin, 1997).
- <sup>3</sup>J. Zaanen, G. A. Sawatzky, and J. W. Allen, *Phys. Rev. Lett.* **55**, 418 (1985).
- <sup>4</sup>M. L. Medarde, *J. Phys.: Condens. Matter* **9**, 1679 (1997).
- <sup>5</sup>J. B. Torrance, P. Lacorre, A. I. Nazzal, E. J. Ansaldo, and C. Niedermayer, *Phys. Rev. B* **45**, 8209 (1992).
- <sup>6</sup>M. Medarde, P. Lacorre, K. Conder, F. Fauth, and A. Furrer, *Phys. Rev. Lett.* **80**, 2397 (1998).
- <sup>7</sup>J. L. Garcia-Munoz, J. Rodriguez-Carvajal, and P. Lacorre, *Europhys. Lett.* **20**, 241 (1992).
- <sup>8</sup>J. Rodriguez-Carvajal, S. Rosenkranz, M. Medarde, P. Lacorre, M. T. Fernandez-Dias, F. Fauth, and V. Trounov, *Phys. Rev. B* **57**, 456 (1998).
- <sup>9</sup>J. A. Alonso, J. L. Garcia-Munoz, M. T. Fernandez-Diaz, M. A. G. Arande, M. J. Martinez-Lope, and M. T. Casais, *Phys. Rev. Lett.* **82**, 3871 (1999).
- <sup>10</sup>P. Lacorre, J. B. Torrance, J. Pannetier, A. I. Nazzal, P. W. Wang, and T. C. Huang, *J. Solid State Chem.* **91**, 225 (1991).
- <sup>11</sup>J. L. Garcia-Munoz, M. Suaaidi, M. J. Martinez-Lope, and J. A. Alonso, *Phys. Rev. B* **52**, 13 563 (1995).
- <sup>12</sup>T. Mizokawa, A. Fujimori, T. Arima, Y. Tokura, N. Mori, and J. Akimitsu, *Phys. Rev. B* **52**, 13 865 (1995).
- <sup>13</sup>This normalization affects the intensity of the raw data by less than 5%.
- <sup>14</sup>The same is true for the intensities [see Fig. 2(c)].
- <sup>15</sup>X. Granados, J. Fontcuberta, X. Obradors, and J. B. Torrance, *Phys. Rev. B* **46**, 15 683 (1992).
- <sup>16</sup>M. Medarde, J. L. Garcia-Munoz, S. Rosenkranz, P. Lacorre, and P. Fischer, *Physica B* **194-196**, 367 (1994).
- <sup>17</sup>T. Katsufuji, Y. Okimoto, T. Arima, Y. Tokura, and J. B. Torrance, *Phys. Rev. B* **51**, 4830 (1995).
- <sup>18</sup>X. Granados, J. Fontcuberta, X. Obradors, J. L. Manosa, and J. B. Torrance, *Phys. Rev. B* **48**, 11 666 (1993).
- <sup>19</sup>M. Medarde, D. Purdie, M. Gironi, M. Hengsberger, Y. Baer, and P. Lacorre, *Europhys. Lett.* **37**, 483 (1997).
- <sup>20</sup>J. L. Garcia-Munoz, J. Rodriguez-Carvajal, P. Lacorre, and J. B. Torrance, *Phys. Rev. B* **46**, 4414 (1992).
- <sup>21</sup>D. D. Sarma, N. Shanthi, S. R. Krishnakumar, T. Saitoh, T. Mizokawa, A. Sekiyama, K. Kobayashi, A. Fujimori, E. Weschke, R. Meier, G. Kaindl, Y. Takeda, and M. Takano, *Phys. Rev. B* **53**, 6873 (1996).
- <sup>22</sup>A. Chainani, H. Kumigashira, T. Takahashi, Y. Tomioka, H. Kuwahara, and Y. Tokura, *Phys. Rev. B* **56**, R15 513 (1997).
- <sup>23</sup>K. Knizek, Z. Jirak, E. Pollert, F. Zounova, and S. Vratilav, *J. Solid State Chem.* **100**, 292 (1992).
- <sup>24</sup>Y. Tomioka, A. Asamitsu, Y. Moritomo, H. Kuwahara, and Y. Tokura, *Phys. Rev. Lett.* **74**, 5108 (1995).
- <sup>25</sup>T. Katsufuji, T. Tanabe, T. Ishikawa, Y. Fukuda, T. Arima, and Y. Tokura, *Phys. Rev. B* **54**, R14 230 (1996).
- <sup>26</sup>R. Mallik, E. V. Sampathkumaran, J. A. Alonso, and M. J. Martinez-Lope, *J. Phys.: Condens. Matter* **10**, 3969 (1998).